NASA TECHNICAL NOTE

NASA TN D-8245

NASA TN D-8245

GRAPHITE AND ABLATIVE MATERIAL RESPONSE TO CO_2-LASER, CARBON-ARC, AND XENON-ARC RADIATION

William D. Brewer

Langley Research Center
Hampton, Va. 23665

NATIONAL AERONAUTICS AND SPACE ADMINISTRATION • WASHINGTON, D. C. • SEPTEMBER 1976

1. Report No. NASA TN D-8245	2. Government Accession No.	3. Recipient's Catalog No.
4. Title and Subtitle GRAPHITE AND ABLATIVE MATERIAL RESPONSE TO CO_2-LASER, CARBON-ARC, AND XENON-ARC RADIATION		5. Report Date September 1976 6. Performing Organization Code
7. Author(s) William D. Brewer		8. Performing Organization Report No. L-10814
9. Performing Organization Name and Address NASA Langley Research Center Hampton, VA 23665		10. Work Unit No. 506-16-21-01 11. Contract or Grant No.
12. Sponsoring Agency Name and Address National Aeronautics and Space Administration Washington, DC 20546		13. Type of Report and Period Covered Technical Note 14. Sponsoring Agency Code
15. Supplementary Notes		

16. Abstract

This study investigated the behavior of graphite and several charring ablators in a variety of high-radiative heat-flux environments. A commercial-grade graphite and nine state-of-the-art charring ablators were subjected to various radiative environments produced by a CO_2 laser and a carbon arc. Graphite was also tested in xenon-arc radiation. Heat-flux levels ranged from 10 to 47 MW/m^2. Tests were conducted in air, nitrogen, helium, and a CO_2-N_2 mixture which simulated the Venus atmosphere. The experimental results were compared with theoretical results obtained with a one-dimensional charring-ablator analysis and a two-dimensional subliming-ablator analysis. Neither the graphite nor the charring ablators showed significant differences in appearance or microstructure after testing in the different radiative environments. The performance of phenolic nylon and graphite was predicted satisfactorily with existing analyses and published material-property data. Good agreement between experimental and analytical results was obtained by using sublimation parameters from a chemical nonequilibrium analysis of graphite sublimation. Some charring ablators performed reasonably well and could withstand radiative fluxes of the level encountered in certain planetary entries. Other materials showed excessive surface recession and/or large amounts of cracking and spalling, and appear to be unsuitable for severe radiative environments.

17. Key Words (Suggested by Author(s)) Ablation Radiation Graphite	18. Distribution Statement Unclassified – Unlimited Subject Category 34		
19. Security Classif. (of this report) Unclassified	20. Security Classif. (of this page) Unclassified	21. No. of Pages 35	22. Price* $3.75

*For sale by the National Technical Information Service, Springfield, Virginia 22161

GRAPHITE AND ABLATIVE MATERIAL RESPONSE TO CO_2-LASER, CARBON-ARC, AND XENON-ARC RADIATION

William D. Brewer
Langley Research Center

SUMMARY

This study investigated the behavior of graphite and several charring ablators in a variety of high-radiative heat-flux environments. A commercial-grade graphite and nine state-of-the-art charring ablators were subjected to various radiative environments produced by a CO_2 laser and a carbon arc. Graphite was also tested in xenon-arc radiation. Heat-flux levels ranged from 10 to 47 MW/m^2. Tests were conducted in air, nitrogen, helium, and a CO_2-N_2 mixture which simulated the Venus atmosphere. The experimental results were compared with theoretical results obtained with a one-dimensional charring-ablator analysis and a two-dimensional subliming-ablator analysis. Neither the graphite nor the charring ablators showed significant differences in appearance or microstructure after testing in the different radiative environments. The performance of phenolic nylon and graphite was predicted satisfactorily with existing analyses and published material-property data. Good agreement between experimental and analytical results was obtained by using sublimation parameters from a chemical nonequilibrium analysis of graphite sublimation. Some charring ablators performed reasonably well and could withstand radiative fluxes of the level encountered in certain planetary entries. Other materials showed excessive surface recession and/or large amounts of cracking and spalling, and appear to be unsuitable for severe radiative environments.

INTRODUCTION

Charring-ablative materials as well as graphite have been used to protect space vehicles from the heating environment encountered during entry into the Earth's atmosphere. The performance of these materials when subjected to environments such as those experienced in Earth entry at orbital and escape velocities has been extensively investigated (refs. 1 to 3). Various analyses have been developed to predict the behavior of materials in such environments (refs. 4 to 9). For proposed planetary missions, however, the problems of protecting the entry vehicles from the severe heating must be reexamined, because in such missions an entry vehicle is subjected to large radiative as well as convective heat inputs. In spite of recent emphasis on the study of these

missions, a better understanding of the interaction of planetary-entry environments and thermal-protection materials is still needed.

Flight tests of each promising thermal-protection material are not feasible and the present capability for simulating planetary-entry environments in ground-based facilities is limited. Certain facilities can produce radiative-and-convective heating of the appropriate levels to simulate some planetary-entry conditions, such as those for selected entries into the Venus atmosphere. Nevertheless, other parameters, such as the spectral distribution of the radiation and the type of atmospheric gases, are in general not well simulated. At present, high-power lasers are the only convenient sources which can produce heat fluxes approaching those expected in entry into the atmospheres of the major planets, but the spectral distribution of radiation produced in these lasers is quite different from that in an actual entry, and the behavior of materials could be different.

A program was therefore undertaken to examine the behavior of graphite and several charring ablators in various radiative heating environments. The objectives of this research were to investigate the important ablative mechanisms and the effect of a change in the environment upon them, to determine the capability of existing ablative analyses to predict satisfactorily material performance in the different environments, and to determine the relative performance of some charring ablators in severe radiative environments.

To carry out this program, a commercial-grade graphite and several charring ablators were subjected to radiative heating environments produced by a CO_2 laser, a carbon arc, and a xenon arc. The experimental results obtained from these tests were compared with theoretical results obtained from two different computer programs which treat the transient response of charring and subliming ablators to heating environments.

SYMBOLS

E	ablative-effectiveness parameter
E^c	ablative-effectiveness parameter based on corrected heat flux
p	pressure
q	local heating rate
q_n	measured heat input less heat reradiated at point of maximum heating
q_{max}	maximum local heating rate

r	radius of sample
s	radial distance from sample center line
T	temperature
Δl	interface recession
Δm	mass loss
Δx	surface recession
ρ	material density

MATERIALS

The materials investigated in the present study (all percentages are by weight) are as follows:

1. A phenolic-carbon (PC) composite of 50 percent phenolic resin and 50 percent carbon fibers, with a density of 1450 kg/m^3
2. A high-density phenolic nylon (HDPN), composed of 50 percent phenolic resin and 50 percent nylon powder, with a density of 1200 kg/m^3
3. A low-density phenolic nylon (LDPN), composed of 25 percent phenolic resin, 25 percent hollow phenolic microspheres, and 50 percent nylon powder, with a density of 550 kg/m^3
4. A silicone elastomer, composed of 75 percent silicone resin, 15 percent SiO_2 (11 percent hollow microspheres and 4 percent fibers), and 10 percent hollow phenolic microspheres, with a density of 640 kg/m^3
5. A filled epoxy material (Apollo heat-shield material), the composition of which is proprietary, with a density of 500 kg/m^3
   (Some measured material properties are given in ref. 10.)
6. A polybenzimidazole (PBI), composed of 69 percent PBI prepolymer, 13 percent carbon fibers, and 18 percent hollow phenolic microspheres (material 5 in ref. 11)
7. A commercial-grade, fine-grained graphite with a density of 1800 kg/m^3
8. A glass-filled Pyrrone resin (P-1) with a density of 600 kg/m^3

9. A foamed Pyrrone (P-2) with a density of 680 kg/m^3

10. An uncured Pyrrone resin (P-3) with a density of 480 kg/m^3

Materials 1 to 7 were tested in the laser facility. Materials 3 to 5 and 7 to 10 were tested in the carbon-arc facility. Only the graphite (material 7) was tested in the xenon-arc facility.

EXPERIMENTAL APPARATUS AND PROCEDURES

Tests were conducted with three different radiation sources: a CO_2 laser, a carbon arc, and a xenon arc. The spectral distributions of the radiation from these sources are shown in figure 1. Figure 1 also presents typical shock-layer radiation spectra for two planetary atmospheres: Earth (air and ablation products) and Venus $(CO_2\text{-}N_2)$. The radiation from the xenon-arc facility and the carbon-arc facility covers a significant portion of the Venus and Earth reentry spectral range. The laser radiation is considerably different from either of the other sources. In addition to being highly coherent and monochromatic, the laser radiation is out of the spectral range of the actual reentry environments. Details of the test apparatus and procedures are given in the following sections.

Laser Experiments

Test apparatus.- The laser used in these experiments was a continuous, dc excited, flowing-gas, CO_2-N_2-He laser operated at Raytheon Research Division, Waltham, Massachusetts. The maximum power output of the device was about 9 kW. For the tests discussed here, the laser was operated at approximately 6 kW with a beam diameter of 4.4 cm. The design, construction, and operating characteristics of the laser are discussed in reference 12.

The test setup used for the laser experiments is shown schematically in figure 2(a). The parallel beam emerged from the laser tube and was reflected by a segmented mirror through a lens onto the surface of a sample located in a test chamber. The energy distribution across the laser beam as it emerged from the tube was not uniform and tended to have a sharp spike near the center, which is typical of high-power laser systems. The segmented mirror randomized or scrambled the beam to produce a more nearly uniform and stable distribution across the surface of the samples. A retractable mirror switched the beam from the sample optics to a calorimeter for calibrating the system. This mirror which was controlled by an electric timer initiated and terminated sample exposure to the laser radiation.

A test chamber maintained a controlled environment about the test samples. Visual observations, motion pictures, and sample temperature measurements were made through side ports. The laser beam passed through a NaCl window in the front of the chamber,

then passed through a 1.3-cm-diameter nozzle, and finally impinged on the sample surface. The test gas, which was injected into a plenum chamber, flowed through the nozzle and past the sample. A vacuum system connected to the rear port removed the test gas and the ablative products and controlled the pressure in the test chamber.

Instrumentation and calibration.- An optical pyrometer measured the temperatures of the test samples. Because the front surface of the samples could not be viewed during a test, the temperature was measured on the side of the samples as close to the front surface as possible. The pyrometer was calibrated to account for the absorption of radiation by the glass viewing window.

One calorimeter, called the primary calorimeter (fig. 2(a)), measured the heat flux at the laser exit. Another calorimeter (not shown) was placed at the rear of the test chamber to measure the heat flux after the beam had been attentuated by the optical system. The intensity distribution across the beam at the test location was determined by exposing polystyrene rods to the laser beam. The rods were sectioned after 0.5 to 1 sec exposure and the intensity profiles were determined from the shapes of the holes burned into the rods.

Test samples, conditions, and procedures.- The test samples for the laser experiments were 0.64-cm-diameter cylinders which were 7.6 cm long. During the tests they were positioned so that about one-third of the length extended out of the holder. The test-sample configuration is shown in figure 2(b). The maximum heat flux at the center of the samples ranged from 36 to 47 MW/m^2. However, the heating was not uniform over the surface of the samples. The heat flux at the edge of the samples ranged from 70 to 80 percent of the maximum depending upon the power output of the laser. A typical heat-flux distribution is given in figure 3.

The gas velocity past the samples of approximately 30 m/sec was sufficient to remove the ablation products from the area of the sample, and the flow was uniform and stable throughout each test. Test gases used were air, nitrogen, and helium.

The samples were placed in the test chamber and the system was regulated to obtain the desired gas flow rate and pressure. The laser was brought to the operating conditions with the retractable mirror reflecting the beam into the primary calorimeter (fig. 2(a)). When the laser had stabilized, the heat flux was recorded and the mirror was removed from the path of the beam to expose the sample to the laser radiation. At the end of the test, the mirror was again inserted into the path of the beam and another heat-flux measurement was made to determine whether or not the laser output had changed during the test. Each sample was measured and weighed before and after each test to determine the surface recession and mass loss. The graphite samples were tested for 5 sec; all other samples were tested for 2 sec.

Carbon-Arc Experiments

Test apparatus.- The tests in carbon-arc radiation were conducted in the arc-image facility at Southwest Research Institute, San Antonio, Texas. The operating characteristics of the facility are given in reference 13. A schematic diagram of the facility as used in this study is shown in figure 4(a). The radiation from a carbon arc was collected and focused onto a test sample by twin parabolic mirrors. The front mirror had a hole in the center, and the door to the facility had a quartz window alined with the mirror hole for viewing the sample during testing. Motion pictures and surface temperature measurements were made through the window. The test samples were enclosed in a small chamber to provide a control of their environment independent of that in the arc chamber. A hemispherical quartz dome formed the front of the test chamber so that the radiation could be focused onto the sample. A graphite disk with a hole in the center was placed in front of the sample to eliminate radiation to the sides of the sample. The test gases were injected through a 1.3-cm-diameter nozzle in front of the sample at a velocity of about 30 m/sec. A vacuum system attached to the rear of the chamber removed the ablative gases and regulated the pressure in the chamber.

A clamshell shutter which was located directly in front of the sample blocked all radiation while the arc facility was being brought to the desired operating conditions. The shutter was controlled by an electronic timer and had opening and closing times of about 0.001 sec.

Instrumentation and calibration.- The heat flux at the sample location was measured with a water-cooled, spherical-cavity, black-body calorimeter. During a calibration run, the calorimeter was placed behind the same shield as the sample so that the calorimeter would collect only the radiation that would be incident on the sample surface. The flux measured by this calorimeter was correlated with that measured by an asymptotic calorimeter located in the beam between the two parabolic mirrors. During a test, only the output of the asymptotic calorimeter was recorded. The heat flux to the sample was determined from these data.

The spatial distribution of the heat flux was determined by placing a block of sodium silicate at the sample location and exposing it to the arc radiation. After the block was exposed to the test environment, it was sectioned and the heating distribution was determined from the shape of the hole burned into the block. In the carbon-arc facility, the variation in heating rate across the sample surface was less than 5 percent.

Surface temperatures were measured with a three-color recording pyrometer as discussed in reference 14. The pyrometer was focused on the front surface of the sample and was calibrated to account for absorption of radiation by the window in the door of the arc chamber and by the quartz dome on the sample chamber.

Test samples, conditions, and procedures.- The test samples were 0.64-cm-diameter, flat-faced cylinders. The measured heat fluxes ranged from 29 to 40 MW/m^2. Yet, the actual heat flux to the surface of the samples was probably much less than that measured. This reduced heat flux is discussed in a subsequent section. Test gases were air, nitrogen, helium, and 90% CO_2-10% N_2. The chamber pressure was varied from 0.3 to 8 atm (1 atm = 0.101325 MPa).

The test samples were positioned in the holder with about two-thirds of the length extending out of the holder (fig. 4(b)). The arc was initiated with the clamshell shutter in the closed position, and the appropriate gas was injected into the sample chamber. When the desired operating conditions had been achieved, the shutter was opened and the sample was exposed for 5 sec. The shutter was then closed to terminate the test. The outputs of the temperature pyrometer and the asymptotic calorimeter were recorded continuously during each test.

Xenon-Arc Experiments

The tests in xenon-arc radiation were conducted in the xenon-lamp apparatus of the high temperature materials laboratory at Langley Research Center. The apparatus consisted of two xenon-arc units focused on a single area. A schematic diagram of the xenon-arc units and the test setup is shown in figure 5(a). The radiation was produced by a xenon arc and was collected and focused by an ellipsoidal mirror. After being focused by the mirror, the radiation passed through an optical integrator to produce a uniform beam. A lens system then refocused the beam onto the sample area. The two lamp units simultaneously irradiated the sample. The center line of each unit made an angle of about 50° with the normal to the sample surface.

The samples were not enclosed in a test chamber. Hence, all tests were in air at 1 atm. A fan removed the ablative products produced during the tests. A recording infrared radiometer which responds to radiation in the 8- to 16-μm wavelength range was used to measure the surface temperatures. Reflection of the arc radiation from the sample surface should therefore not influence the temperature measurement.

The heat flux to the sample as measured by a water-cooled, black-body calorimeter placed in the sample position was correlated with the xenon-arc current which was read directly from meters on the facility control panel. Heat fluxes in these tests were 10 and 11.5 MW/m^2.

The test-sample configuration is shown in figure 5(b). The samples were 1.27-cm-diameter cylinders with a blunted front surface, because such a surface was necessary to obtain a uniform heat flux with the arc units which were arranged as shown in figure 5(a). This shape was determined by exposing Fluorogreen samples to the arc radiation for

various times and determining the equilibrium shape of the surface. The fact that the graphite samples maintained this shape throughout the tests indicated that the heat flux over the front surface was reasonably uniform.

Tests were initiated and terminated with electronically controlled shutters in each arc unit. After the lamps were brought to the operating conditions with the shutters blocking the radiation, they were allowed to stabilize. Then the shutters were opened, the sample was exposed to the radiation for the required length of time, and the shutters were closed to terminate the test. Test times in the xenon arc were 10, 20, 30, and 60 sec.

ANALYSIS

Two different analytical programs were used to make theoretical predictions of the surface and interface recessions for the materials subjected to the heating environments: a one-dimensional charring-ablator program (ref. 6), and a two-dimensional subliming-ablator program (refs. 7 and 8). The one-dimensional numerical analysis was applied for the studies of all materials except the graphite. This charring-ablator program has been employed widely to predict successfully the ablative performance of thermal-protection systems in both ground and flight tests (refs. 15 and 16).

For the graphite studies, the two-dimensional numerical analysis was used. This analysis calculates the transient response of subliming axisymmetric bodies including the effects of shape change. The convective and radiative heat-transfer rates and the pressure distributions around the body are adjusted to account for changes in body geometry. In general, the system which can be analyzed is a single orthotropic material of varying thickness with temperature-dependent thermal properties. The configurations and grid systems used for the two-dimensional calculations are shown in figure 6.

RESULTS AND DISCUSSION

Graphite and charring ablators show different qualitative features during ablation; therefore, different parameters were used to evaluate their performance. Graphite sublimation results in a surface free of degraded material and, thus, the graphite performance was evaluated on the basis of surface recession and mass-loss rates. However, because the charring ablators retain a chemically degraded layer, their performance was evaluated in terms of an ablative-effectiveness parameter (ref. 2) which is based on the maximum depth of material degraded. The ablative-effectiveness parameter is given by the following equation:

$$E = \frac{q_n t}{\rho \, \Delta l}$$

where q_n is the measured heat input (energy/unit time-unit area) less the heat reradiated at the point of maximum heating, t is the test time, ρ is the material density, and Δl is the thickness of material degraded or interface recession. The heat reradiated is computed from the maximum measured surface temperature. The emittance of the test materials in the charred state is taken as 0.9 (ref. 17).

The results from all the tests in all facilities are summarized in tables I and II. Table I gives the results of the charring-ablator tests and table II gives the graphite test results.

Charring Ablator Experiments

Laser tests.- The heat-flux distribution in the laser tests (fig. 3) is, in general, reflected in the shape of the sample surface after testing. The ablator chars for those materials that developed significant char were almost completely hollowed out with only a thin shell of char remaining around the edge. These char shells were fragile and easily broken. Over most of the sample however the interface between the char and the uncharred material was reasonably flat. Apparently, the sides of the material were cooled sufficiently by reradiation to allow a significant amount of char to accumulate. This behavior was typical of both low-density phenolic nylon (LDPN, material 3) and high-density phenolic nylon (HDPN, material 2).

The epoxy material (material 5) showed excessive surface recession with little or no char development. Any char that formed was quickly swept away. The carbon phenolic (PC, material 1) exhibited large amounts of cracking and spalling when exposed to the laser beam. Because large chunks of material flew off and impinged upon the NaCl window in the front of the test chamber, the window failed. Evidently, the differences in thermal-expansion characteristics of the phenolic resin, the carbon fibers, and the carbon formed by the decomposition of the phenolic resin coupled with the very rapid heating caused the failures of the carbon-phenolic materials.

The silicone elastomer (material 4) experienced large surface recessions as well as some bending and twisting during the tests; the performance of the elastomer was comparable to that of the epoxy material. In the two environments in which it was tested, the polybenzimidazole (PBI, material 6) had the greatest effectiveness of any of the charring ablators. A thick, relatively tough char layer developed over most of the front surface. The PBI was however subject to slight surface spallation.

The ablative effectiveness for phenolic nylon and the PBI is shown in figure 7. The LDPN generally performed somewhat better than the HDPN. Neither the chamber pressure nor the test gas had a large effect on the performance of the materials. The materials performed about the same in air, nitrogen, and helium. This behavior probably was

caused by the large quantity of gases generated by the degradation of the material and, thus, the amount of test gas reaching the degrading surface was limited.

Effectiveness values for the phenolic carbon could not be determined because of the severe spallation. The very rapid recession and irregular surfaces of the epoxy and the elastomeric materials made surface temperature and recession measurements questionable at best and no effectiveness values are given. However, if a temperature equal to the sublimation temperature of graphite at the given pressure (refs. 18 and 19) is assumed and an average recession is used, the effectiveness of these two materials is less than one-half that of LDPN.

Carbon-arc tests.- The materials that were tested in both the laser and the carbon-arc facilities (graphite, LDPN, and epoxy) appeared to perform much better in the carbon-arc environment than in the laser environment even though the test conditions were supposed to be approximately the same in both facilities. The mass loss and surface recessions were much smaller and the effectiveness values were much greater. (See tables I and II.) Nonetheless, the actual heat fluxes to the samples in the carbon-arc environment were probably significantly less than those measured because of the absorption of incoming radiation by the ablative gases. The sample chamber and gas flow arrangement (fig. 4) were such that the ablative gases were not swept away cleanly and a significant volume of gas built up in front of the sample.

Figure 8 shows the spectral absorption coefficient for a carbon plasma at 3000 K and 1 atm (from ref. 20). For comparison, the spectral-energy distribution of the carbon arc is superimposed on the absorption-coefficient curve. Over almost the entire spectral range of the carbon-arc radiation, the absorption coefficient is significant and approaches 100 cm^{-1}. Thus, the heat flux to the sample could be reduced substantially by the absorption of arc radiation by the ablative gases. A corrected heat flux was determined for all carbon-arc tests by assuming that the absorption coefficient of the ablative gases was 1 cm^{-1} and that the equivalent of 1 cm of absorbing gases was in front of each test sample. The results then agree more closely with the laser test results and with the calculations to be discussed.

Figure 9 gives the ablative effectiveness (corrected heat flux) for the ablators tested in a carbon-arc environment. The LDPN material and the P-3 material (material 10) performed best with effectiveness values in the range of those for the laser tests. The P-1 and P-2 materials (materials 8 and 9) had greater interface recession in spite of their higher densities and hence had low effectiveness. Again, the elastomer and the epoxy material had relatively large recession rates. The LDPN material performed slightly better in inert atmospheres than in air. The LDPN, elastomer, and epoxy materials behaved about the same in air as in the CO_2-N_2 atmosphere. Changes in pressure over the range considered had no apparent effect on material effectiveness.

The LDPN, P-2, and P-3 materials developed relatively thick chars over the surface and showed little or no front surface recession around the edge. The surfaces were cupped slightly in the central area because of the radiative cooling around the sides. The interface between the char and the uncharred material was weak and the char tended to separate from the sample. This weak interface is also typical of the LDPN material when it is tested in low-convective heat-flux environments.

The P-1 material had a very thin (less than 1 mm) fully developed char and a somewhat larger depth of partially degraded material. The char was tough and strongly attached. Although the effectiveness of P-1 was rather low, the physical appearance and surface integrity were better than those of the other ablators.

Graphite Experiments

Table II gives a summary of all the graphite test results. Material performance was evaluated on the basis of mass-loss rates and/or surface recessions.

Mass-loss-rate data for the various environments are given in figure 10. For the laser tests, the rates were based on surface recession at the center of the sample front surface. In these tests, the graphite performed about the same in nitrogen as in helium. Also, changes in pressure from 0.1 to 1.0 atm did not affect material performance and mass-loss rates were greater in air than in the other gases.

For the carbon-arc tests, the mass-loss rates were based on sample weights before and after testing because the surface recessions were too small to measure. The symbols in figure 10 indicate the average values since variations in incident heat flux caused some data scatter. The mass-loss rates for the carbon-arc tests were much less than those in the laser tests, even though the measured heat fluxes were comparable. The results are more consistent if a corrected heat flux (discussed previously for the charring ablator, carbon-arc tests) is used. Then the results also agree reasonably well with those of reference 21 as well as with the analytical results to be discussed. The graphite behavior was essentially the same in air and in the CO_2-N_2 gas mixture. In each gas at pressures from 1 to 8 atm, the trend was for greater mass-loss rates at higher pressures. (Ref. 22 reports a correlation in which the mass-loss rate of graphite is directly proportional to the pressure.)

The results of the xenon-arc tests are given in table II. In these relatively low heat-flux tests, the samples were studied for times ranging from 10 to 60 sec, so that appreciable surface recession could be obtained. No heat-flux correction was necessary because the test configuration did not cause significant buildup of gases in front of the test samples. Calculated surface recessions correspond favorably with the experimental values as shown in the next section.

Analytical Results

Calculations were made for only graphite and phenolic nylon because these materials are well characterized and their thermophysical properties are best known. Also, the analyses used cannot treat the mechanical removal of material such as occurred with several of the materials tested. The thermophysical properties of phenolic nylon were obtained from reference 10 and those of graphite from reference 23. The sublimation parameters were obtained from references 21 and 24. The analysis of reference 24 is a simplified chemical-nonequilibrium treatment of charring ablator and graphite sublimation and yields results which are in good agreement with the experimental results of reference 22.

Figure 11(a) presents the experimental and calculated results for one graphite test in the laser facility in air at a pressure of 1 atm with a heat flux of 45.8 MW/m^2. The calculated surface recession at the end of a 5-sec test is compared with the measured values. The scale on the ordinate is inverted so that the curves shown indicate the actual shape of the front surface from the sample center line (s/r = 0) to the sample edge (s/r = 1). The dashed line indicates the initial shape of the sample. The agreement between the calculated and experimental results is, in general, reasonably good. Although the results differ at the sample center line, the magnitude of this difference is only about 0.5 mm. Attempts to lessen the difference by invoking mass-loss mechanism other than sublimation and oxidation were unsuccessful. Absorption of radiation below the front surface with subsequent periodic explosive mass removal could lead to greater recession, as could preferential ablation of the graphite binder. However, in the present graphite tests, no significant particulate removal was observed. Phenomena such as electric field effects associated with intense laser beams, direct interaction of photons with atoms and molecules to dissociate carbon-carbon bonds, and multiphoton effects are possible contributors to additional mass loss (ref. 25). They are however unusual effects and simple analysis indicates that the associated mass-loss rates are negligible compared with those observed. Some typical results for graphite tests in nitrogen and helium atmospheres in the laser facility are shown in figures 11(b) and 11(c). For these tests, the agreement between the calculated and experimental results is very good.

Figure 12 shows typical results for graphite tests in air in the carbon-arc facility. Two sets of calculations are compared with the experimental results. The calculations in which the measured heat flux was used predict large recession rates, but the tests showed no measurable recession. If the corrected heat flux is used, the calculations then show negligible recession and are in agreement with the experiment. Similar results were obtained for all other test gases in the carbon-arc facility.

Further evidence that the heat flux to the ablating samples in the carbon arc was much less than that measured in the absence of ablation is given by the low-density

phenolic-nylon results shown in table III and in figure 13. Histories of the calculated stagnation-point surface and interface recessions are given for both the measured heat flux and the corrected heat flux of tests in air at various pressures. Both the surface and interface total recessions calculated using the corrected heat flux agree very well with the measured values. These calculations were made with the one-dimensional charring-ablator analysis of reference 6.

Results for the graphite tests in the Xenon-arc facility are given in figure 14. Histories of the stagnation-point surface recession are shown for the two heat fluxes. Again, the two-dimensional sublimation analysis satisfactorily predicts the material response.

CONCLUDING REMARKS

This investigation studied the behavior of graphite and several charring ablators in various high-radiative heat-flux environments produced by a CO_2 laser, a carbon arc, and a xenon arc. Heat-flux levels ranged from 10 to 47 MW/m^2. The experimental results were compared with theoretical calculations.

The performance of phenolic nylon and graphite in the radiative environments was satisfactorily predicted with existing analyses and published material-property data. Good agreement between experimental and analytical results was obtained with constants derived from a simplified chemical nonequilibrium analysis of graphite sublimation.

The low-density phenolic nylon and the polybenzimidazole performed reasonably well in the high-radiative heat fluxes. The epoxy material (Apollo heat-shield material) and the silicone elastomer showed excessive surface recession in all test conditions and appear to be unsuitable for the severe radiative environments. When exposed to the laser radiation, the carbon-phenolic composite showed large amounts of cracking and spalling, apparently because of differential thermal expansion between the phenolic resin and the carbon fibers.

In the laser tests, the charring ablators behaved about the same in air, nitrogen, and helium. In the carbon-arc tests, the low-density phenolic-nylon material performed slightly better in nitrogen and helium than in air, but the differences in performance were small. The materials also performed about the same in 90% CO_2-10% N_2 as in air. Variations in chamber pressure over the range 0.1 to 3.0 atm had no significant effect on the performance of the charring ablators.

Differences in graphite mass-loss rates in nitrogen and in helium were negligible. Graphite also performed about the same in air as in 90% CO_2-10% N_2 with mass-loss rates somewhat greater than in nitrogen or helium. Variation in pressure from 0.1 to 1.0 atm did not affect the performance of graphite; whereas, in the pressure range from

1 to 8 atm, the trend was for greater mass-loss rates at higher pressures. This trend was seen in both air and in CO_2-N_2.

Langley Research Center
National Aeronautics and Space Administration
Hampton, VA 23665
June 16, 1976

REFERENCES

1. Dow, Marvin B.; and Brewer, William D.: Performance of Several Ablation Materials Exposed to Low Convective Heating Rates in an Arc-Jet Stream. NASA TN D-2577, 1965.

2. Swann, Robert T.; Brewer, William D.; and Clark, Ronald K.: Effect of Composition, Density, and Environment on the Ablative Performance of Phenolic Nylon. NASA TN D-3908, 1967.

3. Tompkins, Stephen S.; and Kabana, Walter P.: Effects of Material Composition on the Ablation Performance of Low-Density Elastomeric Ablators. NASA TN D-7246, 1973.

4. Moyer, Carl B.; and Rindal, Roald A.: An Analysis of the Coupled Chemically Reacting Boundary Layer and Charring Ablator. Part II – Finite Difference Solution for the In-Depth Response of Charring Materials Considering Surface Chemical and Energy Balances. NASA CR-1061, 1968.

5. Scala, Sinclaire M.; and Gilbert, Leon M.: Thermal Degradation of a Char-Forming Plastic During Hypersonic Flight. ARS J., vol. 32, no. 6, June 1962, pp. 917-924.

6. Swann, Robert T.; Pittman, Claud M.; and Smith, James C.: One-Dimensional Numerical Analysis of the Transient Response of Thermal Protection Systems. NASA TN D-2976, 1965.

7. Tompkins, Stephen S.; Moss, James N.; Pittman, Claud M.; and Howser, Lona M.: Numerical Analysis of the Transient Response of Ablating Axisymmetric Bodies Including the Effects of Shape Change. NASA TN D-6220, 1971.

8. Howser, Lona M.; and Tompkins, Stephen S.: Computer Program for the Transient Response of Ablating Axisymmetric Bodies Including the Effects of Shape Change. NASA TM X-2375, 1971.

9. Scala, Sinclaire M.; and Gilbert, Leon M.: Sublimation of Graphite at Hypersonic Speeds. AIAA J., vol. 3, no. 9, Sept. 1965, pp. 1635-1644.

10. Wilson, R. Gale, compiler: Thermophysical Properties of Six Charring Ablators From 140° to 700° K and Two Chars From 800° to 3000° K. NASA TN D-2991, 1965.

11. Dickey, Robert R.; Lundell, John H.; and Parker, John A.: The Development of Polybenzimidazole Composites as Ablative Heat Shields. J. Macromol. Sci. – Chem., vol. A3, no. 4, July 1969, pp. 573-584.

12. Horrigan, F. A.; Klein, C. A.; Rudko, R. I.; and Wilson, D. T.: High Power Gas Laser Research. S-1084 (Contract No. DA-AH01-67-C-1589), Res. Div., Raytheon Co., Sept. 1968.

13. Cook, John C.: A Four-Hundred Kilowatt Pressurized Arc Imaging Furnace. Thermal Imaging Techniques, Peter E. Glaser and Raymond F. Walker, eds., Plenum Press, 1964, pp. 55-76.

14. Baker, E. Jack, Jr.: Determination of Surface Temperature and Emissivity. Final Rep., Project 02-1862, Southwest Res. Inst., May 13, 1966.

15. Olsen, George C.; and Chapman, Andrew J., III: Flight and Ground Tests of a Very-Low-Density Elastomeric Ablative Material. NASA TN D-6956, 1972.

16. Brewer, William D.; and Kassel, Philip C., Jr.: Flash X-Ray Technique for Investigating Ablative Material Response to Simulated Re-Entry Environments. Int. J. Non-Destruct. Test., vol. 3, no. 4, 1972, pp. 375-390.

17. Wilson, R. Gale: Hemispherical Spectral Emittance of Ablation Chars, Carbon, and Zirconia to 3700° K. NASA TN D-2704, 1965.

18. Glockler, George: The Heat of Sublimation of Graphite and the Composition of Carbon Vapor. J. Chem. Phys., vol. 22, no. 2, Feb. 1954, pp. 159-161.

19. Zavitsanos, P. D.: Mass Spectrometric Analysis of Carbon Species Generated by Laser Evaporation. Carbon, vol. 6, no. 5, Oct. 1968, pp. 731-737.

20. Nelson, H. F.: Radiative Transfer Through Carbon Ablation Layers. J. Quant. Spectry. & Radiat. Transfer, vol. 13, no. 5, May 1973, pp. 427-445.

21. Davy, William C.; and Bar-Nun, Akiva: Vaporization Characteristics of Carbon Heat Shields Under Radiative Heating. AIAA Paper No. 72-296, Apr. 1972.

22. Bishop, W. M.; and Dicristina, V.: The Combustion and Sublimation of Carbon at Elevated Temperatures. AIAA Paper No. 68-759, June 1968.

23. Wakefield, Roy M.; and Peterson, David L.: Graphite Ablation in Combined Convective and Radiative Heating. J. Spacecr. & Rockets, vol. 10, no. 2, Feb. 1973, pp. 149-154.

24. Balhoff, John F.; and Pike, Ralph W.: Modeling Sublimation of a Charring Ablator. J. Spacecr. & Rockets, vol. 10, no. 12, Dec. 1973, pp. 822-824.

25. Ensign, Thomas C.; and Lye, Robert G.: Effects of Intense Ultraviolet Radiation on Carbonaceous Ablative Heat Shields. RIAS Tech. Rep. 71-23, Martin Marietta Corp., Oct. 1971.

TABLE I.- CHARRING ABLATOR TEST RESULTS

Facility	Material	Test gas	Pressure, atm	Heat flux, MW/m^2		Surface temperature, K	Test time, sec	Δx, cm	Δl, cm	Δm, g	E, MJ/kg	E^c, MJ/kg
				Measured	Corrected							
Laser	LDPN	Air	0.1	42.0	---	3130	2	---	0.560	0.164	24.1	---
			.3	42.0	---	3520		---	.510	.145	24.4	---
			1.0	42.6	---	3350		---	.460	.162	28.6	---
		N_2	.1	40.5	---	3520		---	.560	.170	21.2	---
			.3	41.1	---	3280		---	.460	.122	27.8	---
			1.0	40.6	---	3390		---	.430	.140	28.6	---
		He	.1	41.0	---	3660		---	.560	.162	20.7	---
			.3	36.5	---	3180		---	.406	.113	28.0	---
			1.0	45.9	---	3290		---	.406	.103	35.8	---
	HDPN	Air	0.1	42.0	---	2940	2	---	0.305	0.127	21.8	---
			.3	42.0	---	3580		---	.330	.209	17.7	---
			1.0	42.0	---	3300		---	.330	.210	19.0	---
			1.0	43.5	---	3280		---	.305	.126	21.4	---
		N_2	.1	41.8	---	3520		---	.305	.123	19.4	---
			.3	41.9	---	3110		---	.305	.092	21.2	---
			1.0	40.7	---	3450		---	.280	.099	20.8	---
		He	.1	41.0	---	3660		---	.254	.116	21.8	---
			.3	36.1	---	3180		---	.254	.082	21.1	---
			1.0	43.3	---	3300		---	.254	.084	25.5	---

TABLE I.- Continued

Facility	Material	Test gas	Pressure, atm	Heat flux, MW/m^2		Surface temperature, K	Test time, sec	Δx, cm	Δl, cm	Δm, g	E, MJ/kg	E^c, MJ/kg
				Measured	Corrected							
Laser	PC	Air	0.1	43.0	---	---	2	---	----	0.103	---	---
			.3	41.0	---	---		---	----	.088	---	---
			.3	42.5	---	---		---	----	.098	---	---
			1.0	42.0	---	---		---	----	.135	---	---
			1.0	43.0	---	---		---	----	.124	---	---
			1.0	43.3	---	---		---	----	.108	---	---
		N_2	.1	40.5	---	---		---	----	.043	---	---
			.3	42.3	---	---		---	----	.066	---	---
			1.0	40.7	---	---		---	----	.068	---	---
		He	.1	40.8	---	---		---	----	.046	---	---
			.3	36.2	---	---		---	----	.068	---	---
	"		1.0	36.6	---	---	"	---	----	.089	---	---
	Epoxy	Air	0.1	42.0	---	---	2	---	----	0.213	---	---
			.3	41.0	---	---		---	1.13	.179	---	---
			1.0	42.0	---	---		---	1.45	.239	---	---
		N_2	.1	40.0	---	---		---	----	.238	---	---
		N_2	.3	39.0	---	---		---	1.33	.159	---	---
		He	.1	40.0	---	---		---	1.33	.161	---	---
		He	.3	37.0	---	---		---	1.18	.142	---	---
	PBI	Air	0.1	40.0	---	3110	2	---	0.410	0.056	34.4	---
	PBI	N_2	.1	41.0	---	3150		---	.410	.081	28.2	---
	Elastomer	Air	.1	42.0	---	---		---	1.270	.192	---	---
"	Elastomer	N_2	.1	40.0	---	---		---	1.270	.252	---	---

TABLE I.- Concluded

Facility	Material	Test gas	Pressure, atm	Heat flux, MW/m^2		Surface temperature, K	Test time, sec	Δx, cm	Δl, cm	Δm, g	E, MJ/kg	E^c, MJ/kg
				Measured	Corrected							
Carbon arc	LDPN	Air	0.3	33.4	12.3	3213	5	0.050	0.305	0.064	83.4	20.4
			1.0	40.3	14.8	3203		.050	.406	.083	78.2	21.2
			3.0	35.5	13.1	3113		.030	.356	.070	78.4	21.2
			3.0	34.7	12.8	3043		.030	.305	.084	90.4	25.0
		N_2	1.0	39.0	14.3	3163		.050	.305	.073	101.0	27.5
		He	1.0	37.7	13.9	3173		.050	.330	.077	89.6	24.0
		CO_2-N_2	1.0	30.4	11.2	2993		.050	.279	.051	85.7	23.1
		CO_2-N_2	3.0	32.9	12.1	3113		.100	.305	.071	83.8	25.8
	Epoxy	Air	1.0	33.4	12.3	3043	5	0.040	0.660	0.090	43.1	11.8
	Epoxy	CO_2-N_2	3.0	35.5	13.1	2823	5	.290	.587	.090	53.9	16.4
	Elastomer	Air	1.0	33.4	12.3	3003	5	0.870	1.14	0.069	53.4	14.9
		Air	3.0	36.0	13.2	3003		.870	1.55	.069	42.6	12.0
		CO_2-N_2	3.0	33.8	12.4	3023		.770	1.12	.062	54.9	15.2
	P-1	Air	1.0	32.1	11.8	3073	5	0.280	0.406	0.047	56.6	14.8
	P-2			33.4	12.3	3153		.050	.508	.040	41.1	10.5
	P-3			37.4	12.8	3093		.070	.381	.035	82.1	22.1

TABLE II.- GRAPHITE TEST RESULTS

Facility	Test gas	Pressure, atm	Heat flux, MW/m^2		Surface temperature, K	Test time, sec	Δx, cm	Δm, g
			Measured	Corrected				
Laser	Air	0.1	42.0	---	3615	5	0.203	0.073
↓	↓	.1	42.0	---	3619	↓	.204	.073
		.3	42.0	---	3530		.191	.069
		.3	42.0	---	3400		.186	.067
		1.0	45.8	---	3345		.203	.073
	↓	1.0	44.2	---	3345	↓	.185	.067
	N_2	0.1	40.0	---	2900	5	0.102	0.006
	↓	.1	41.6	---	2865	↓	.102	.005
		.1	45.8	---	2860		.102	.004
		.1	47.0	---	2850		.110	.008
		.3	42.1	---	2865		.102	.006
		.3	41.4	---	3080		.089	.005
		1.0	42.0	---	3500		.110	.020
	↓	1.0	40.8	---	3400	↓	.102	.016
	He	0.3	39.2	---	----	5	0.102	0.011
	↓	.3	37.7	---	2650	↓	.089	.004
		1.0	38.0	---	3080		.102	.011
↓	↓	1.0	38.8	---	3185	↓	.114	.012

TABLE II.- Continued

Facility	Test gas	Pressure, atm	Heat flux, MW/m^2		Surface temperature, K	Test time, sec	Δx, cm	Δm, g
			Measured	Calculated				
Carbon arc	Air	0.3	37.2	13.7	3600	5	0	0.005
		1.0	42.5	15.6	3800			.008
			35.5	13.1	3690			.003
			32.5	12.0	3540			.003
			34.1	12.5	3590			.005
			34.0	12.5	3600			.004
			27.4	10.1	3070			.004
			32.0	11.8	3540			.006
		3.0	34.2	12.6	3490			.011
			33.4	12.3	3400			.005
			30.4	11.2	3500			.004
			34.9	12.8	3440			.006
		5.0	34.9	12.8	3580			.010
			38.7	14.2	3740			.010
			35.7	13.1	3590			.011
			34.7	13.8	3800			.010
		8.0	28.8	10.6	2880			.014
			32.4	12.0	3240			.014
			30.0	11.0	3000			.015
			31.8	11.7	3180			.013

TABLE II.- Concluded

Facility	Test gas	Pressure, atm	Heat flux, MW/m^2		Surface temperature, K	Test time, sec	Δx, cm	Δm, g
			Measured	Corrected				
Carbon arc	CO_2-N_2	1.0	32.0	11.8	3370	5	0	0.004
		3.0	37.6	13.8	3680			.006
		3.0	38.2	14.0	3650			.005
		5.0	34.5	12.7	3760			.010
		5.0	33.5	12.3	3700			.009
		5.0	33.0	12.0	3670			.010
		5.0	29.7	11.0	3300			.006
Xenon arc	Air	1.0	11.5		2650	10	0.008	0.103
					2800	20	.018	.159
					2600	20	.018	.325
					2850	30	.024	.220
					3000	30	.025	.129
			10.0		2600	30	.020	.207
			10.0		2800	60	.039	----

TABLE III.- LOW-DENSITY PHENOLIC-NYLON CALCULATIONS

Facility	Test gas	Pressure, atm	Heat flux, MW/m^2	Time, sec	Δl, cm		Δx, cm	
					Calculated	Experimental	Calculated	Experimental
Carbon arc	Air	0.3	33.4	5	0.585	----	0.329	---
↓	↓	.3	[a]12.3	↓	.407	0.305	.012	0.05
		1.0	40.3		.667	----	.459	---
		1.0	[a]14.8		.428	.406	.029	.05
		3.0	35.5		.607	----	.367	---
		3.0	[a]13.0		.413	.356	.015	.03

[a]Corrected heat flux.

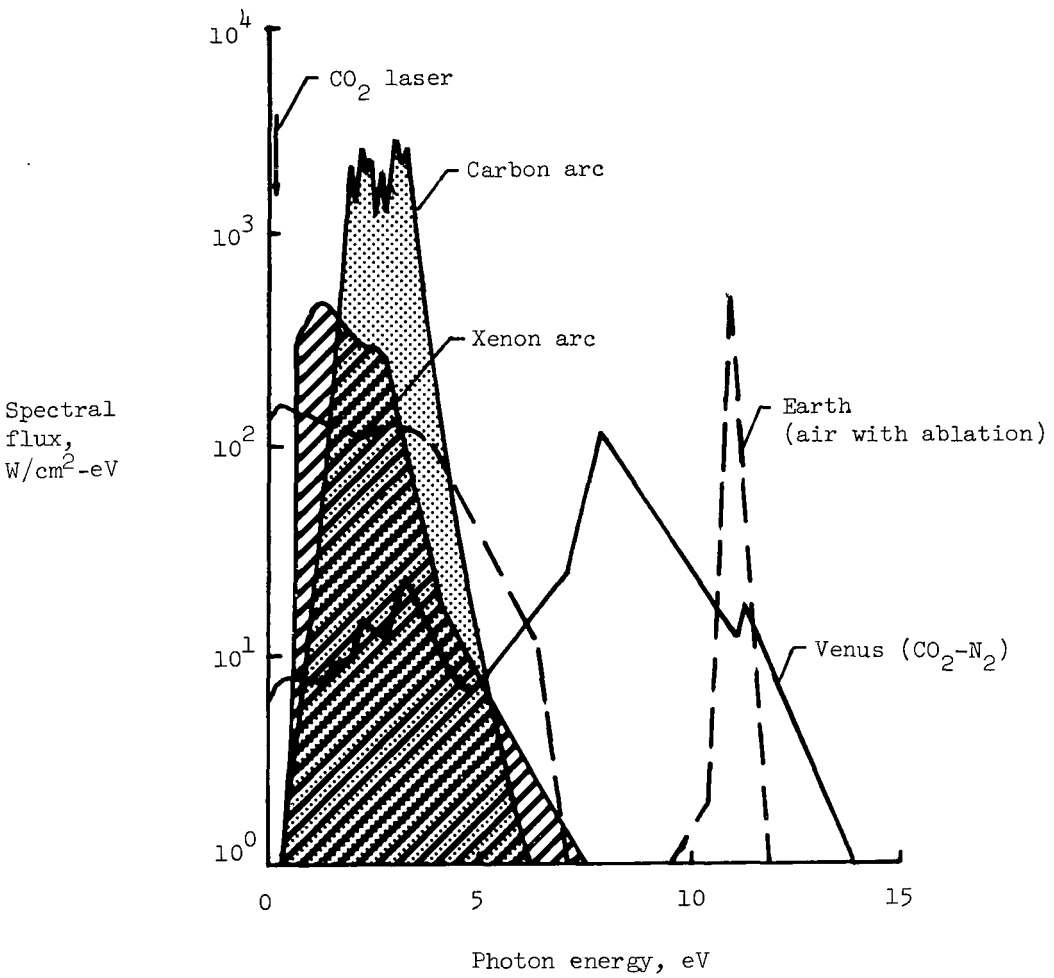

Figure 1.- Shock-layer spectra for Earth and Venus atmospheres and spectra for ground test facilities.

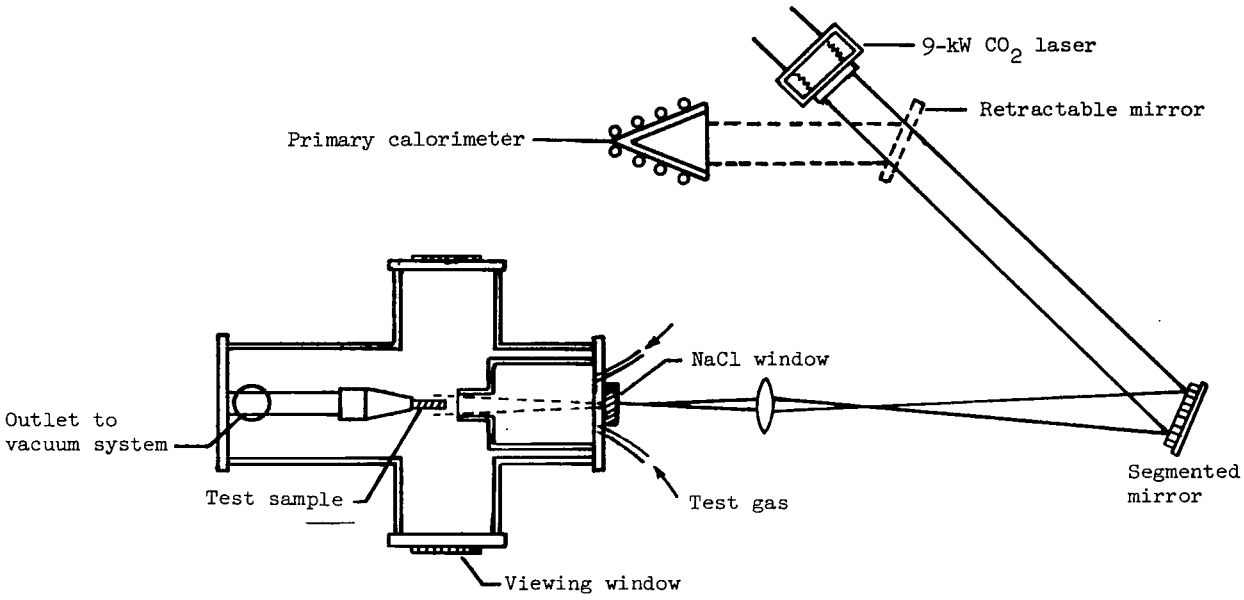

(a) Test setup.

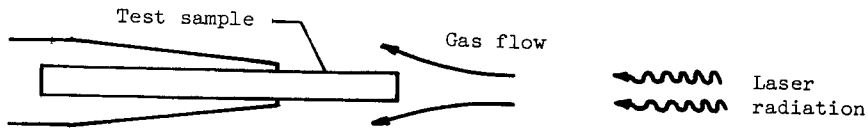

(b) Test-sample configuration.

Figure 2.- Laser experiments.

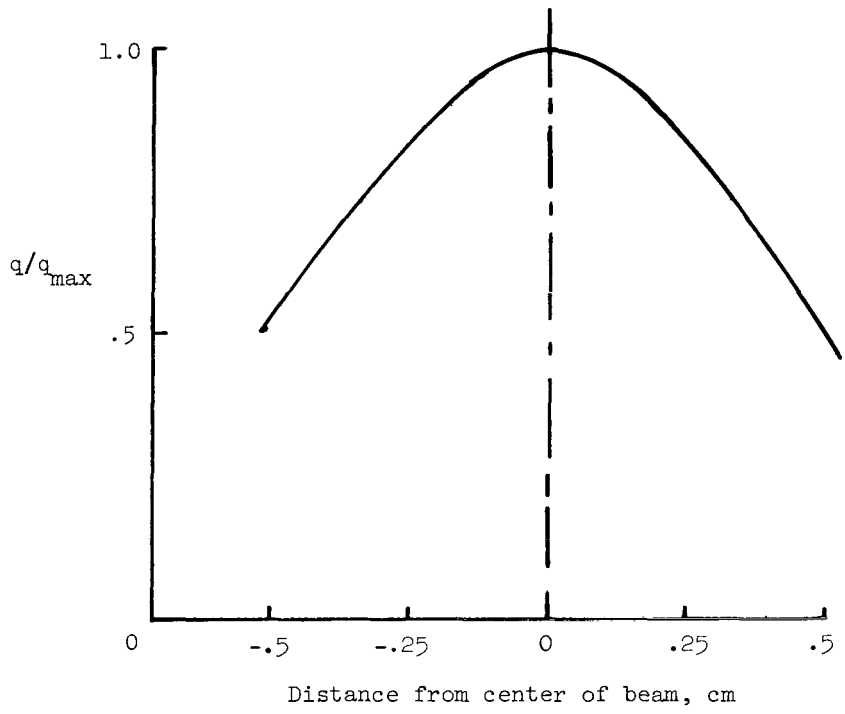

Figure 3.- Typical heat-flux distribution in laser facility.

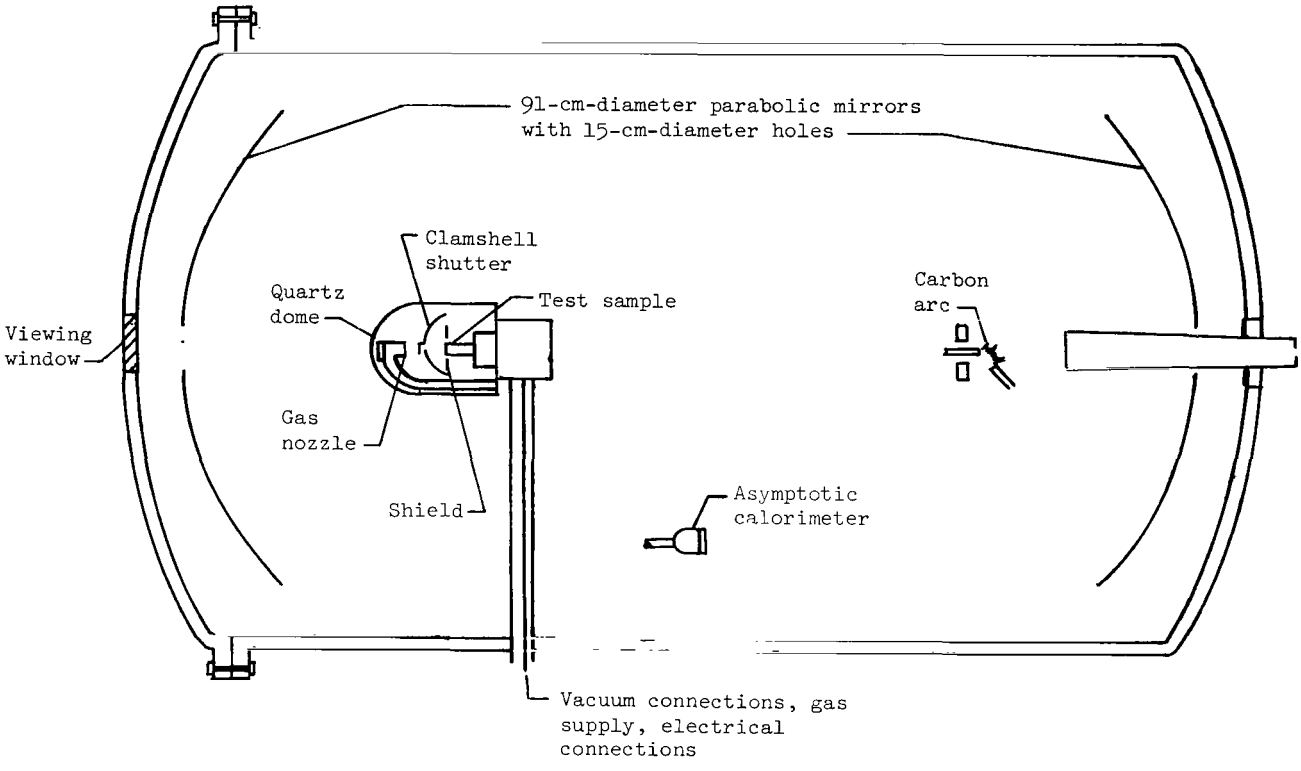

(a) Test setup.

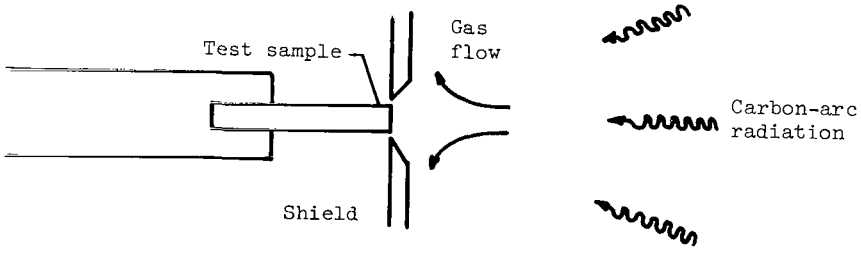

(b) Test-sample configuration.

Figure 4.- Carbon-arc experiments.

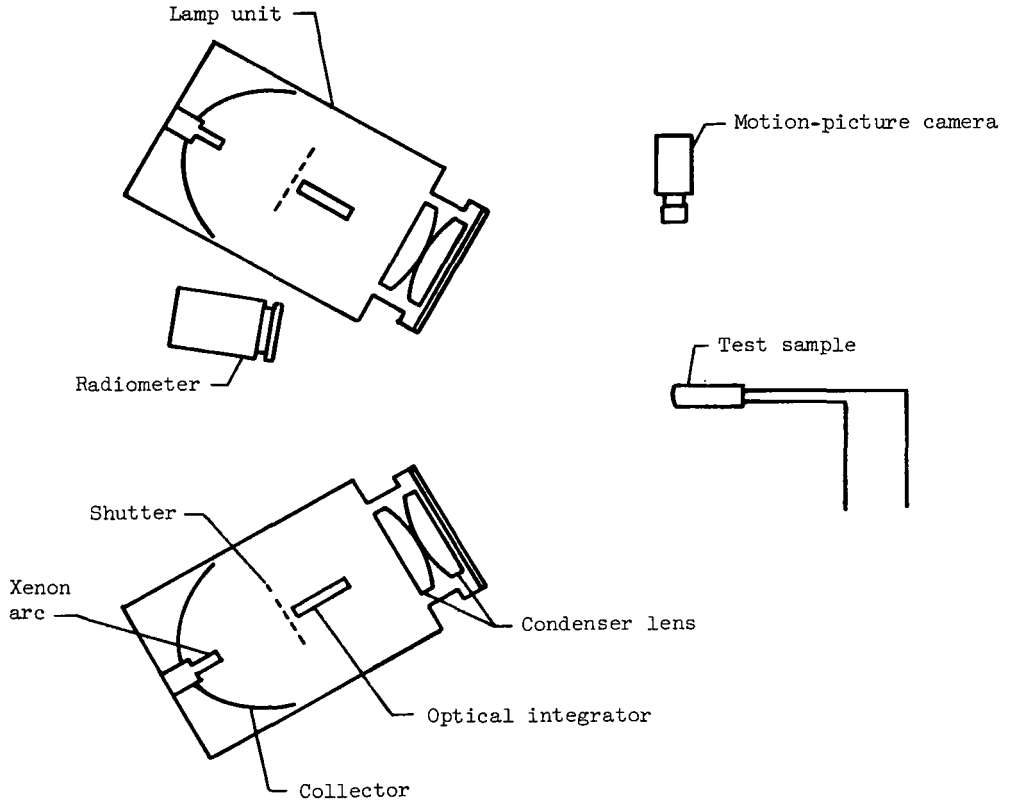

(a) Test setup.

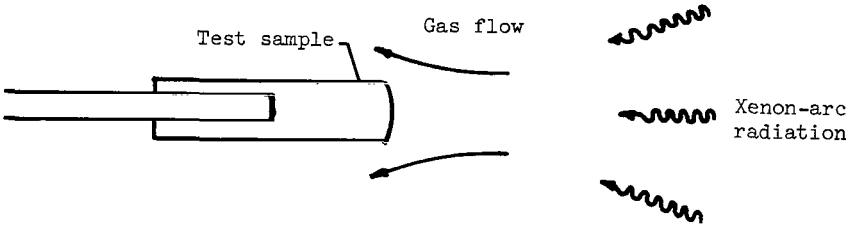

(b) Test-sample configuration.

Figure 5.- Xenon-arc experiments.

(a) Blunt model (xenon-arc samples).

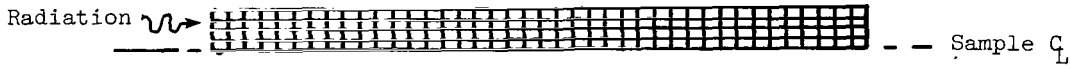

(b) Flat model (laser and carbon-arc samples).

Figure 6.- Numerical grid systems for two-dimensional calculations.

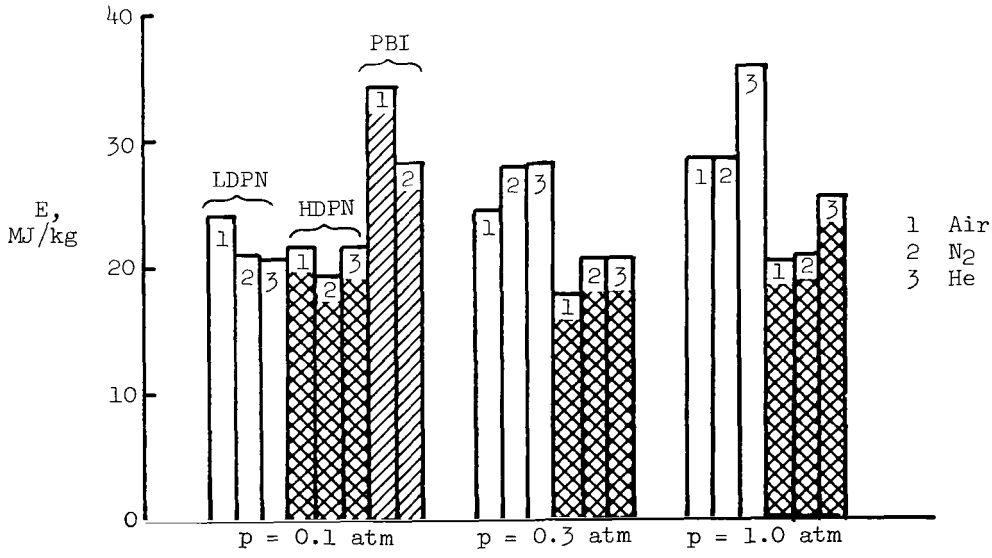

Figure 7.- Ablative effectiveness of charring materials in laser experiments.

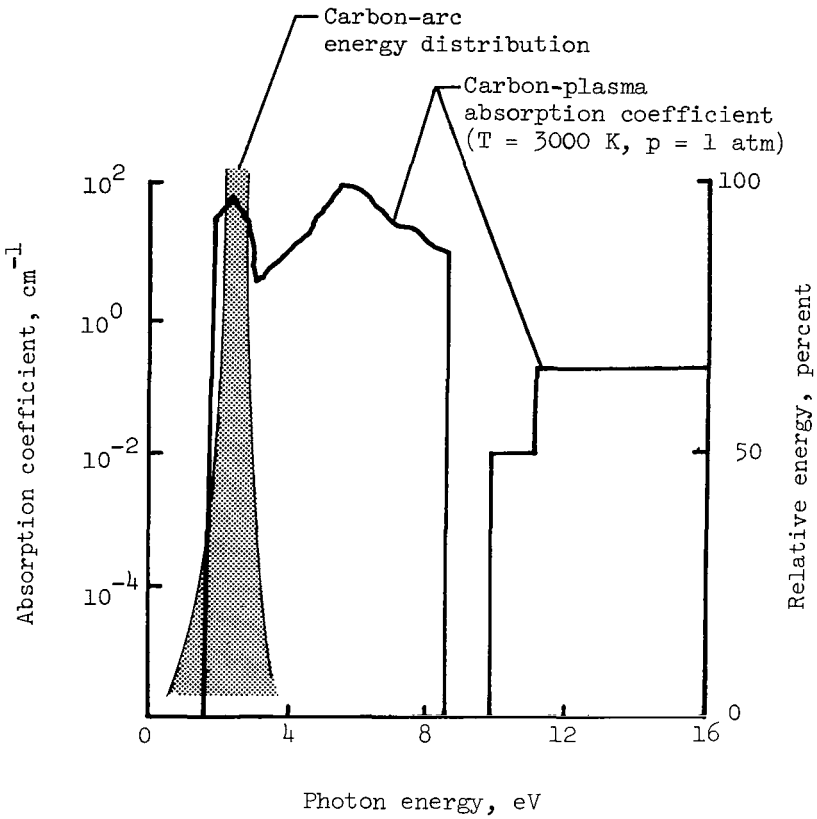

Figure 8.- Spectral distributions of carbon-plasma absorption coefficient and carbon-arc energy output.

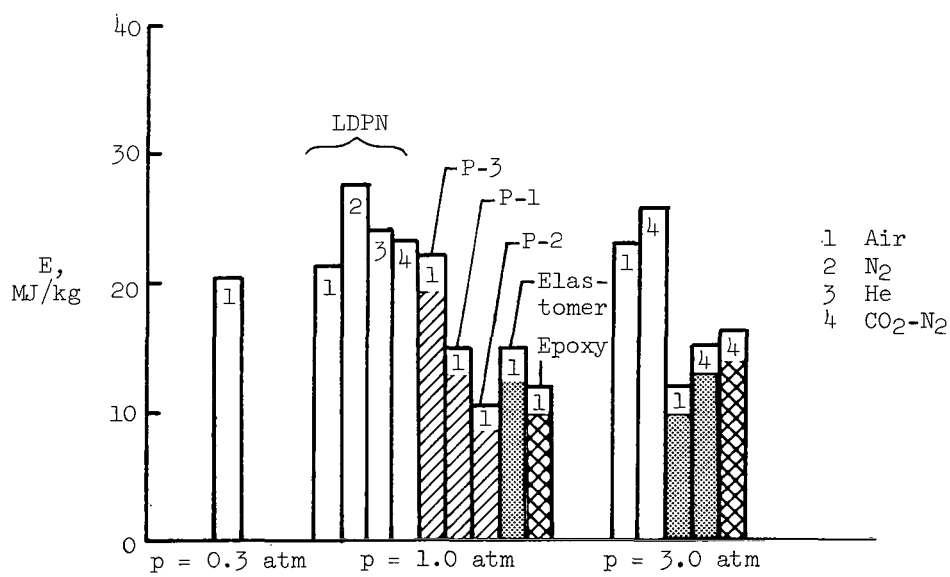

Figure 9.- Ablative effectiveness of charring materials in carbon-arc environments (corrected heat flux).

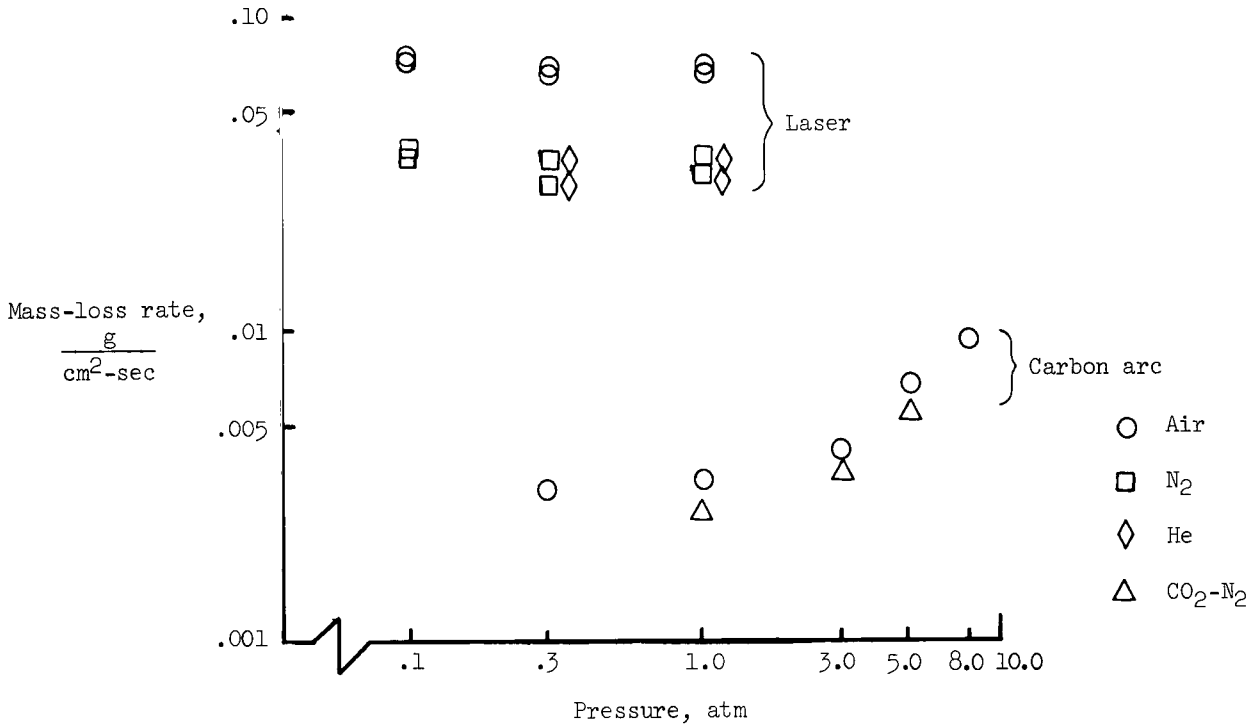

Figure 10.- Experimental mass-loss rates for graphite.

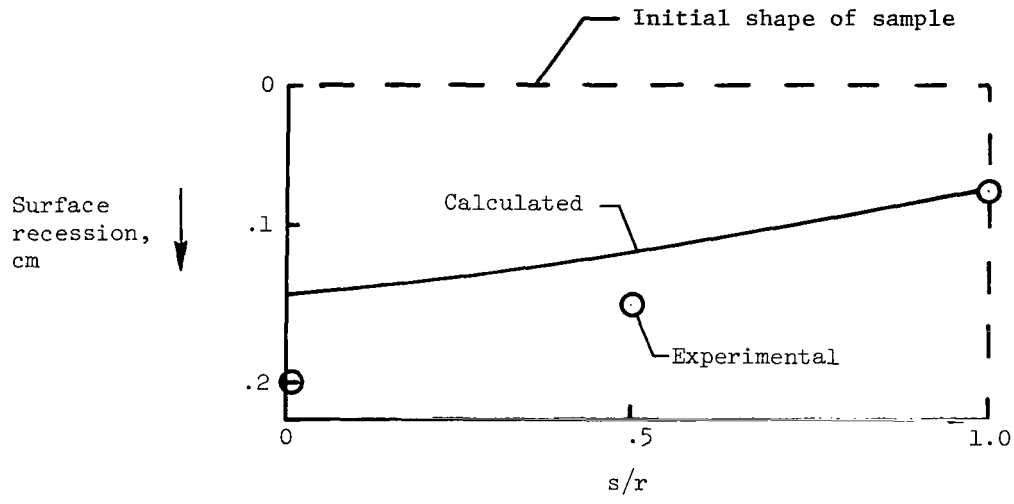

(a) Air; p = 1 atm; heat flux, 45.8 MW/m^2.

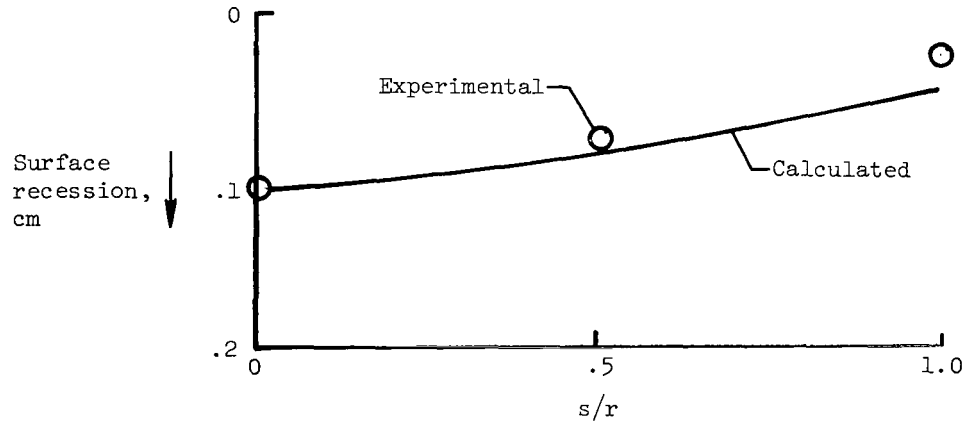

(b) Nitrogen; p = 1 atm; heat flux, 40.8 MW/m^2.

Figure 11.- Experimental and calculated graphite recession in laser facility.

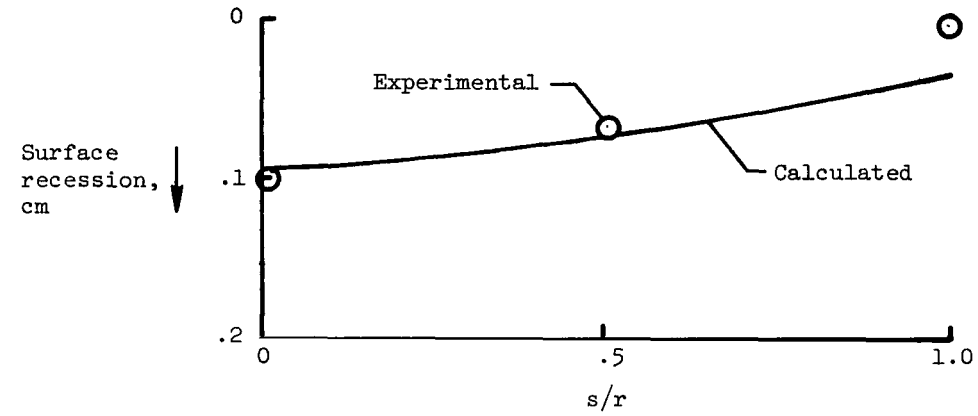

(c) Helium; p = 1 atm; heat flux, 38.0 MW/m^2.

Figure 11.- Concluded.

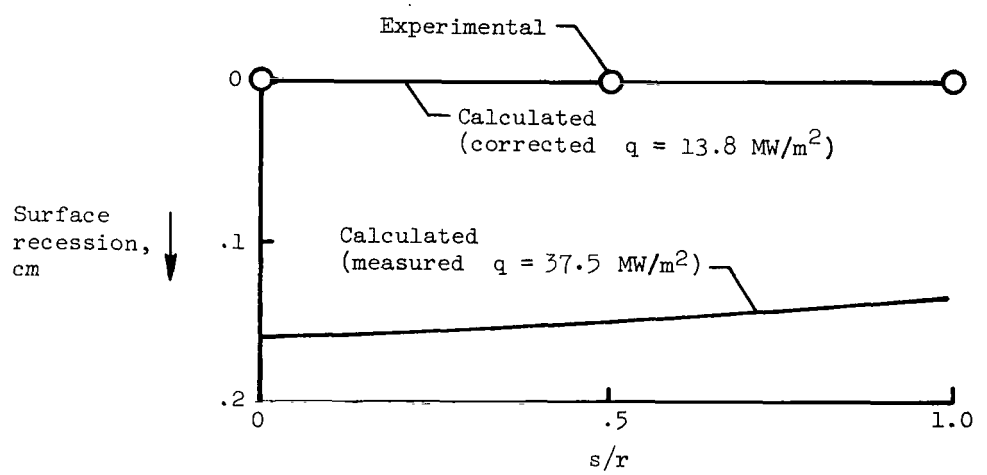

Figure 12.- Experimental and calculated recessions for graphite in carbon-arc facility. Air; p = 1 atm.

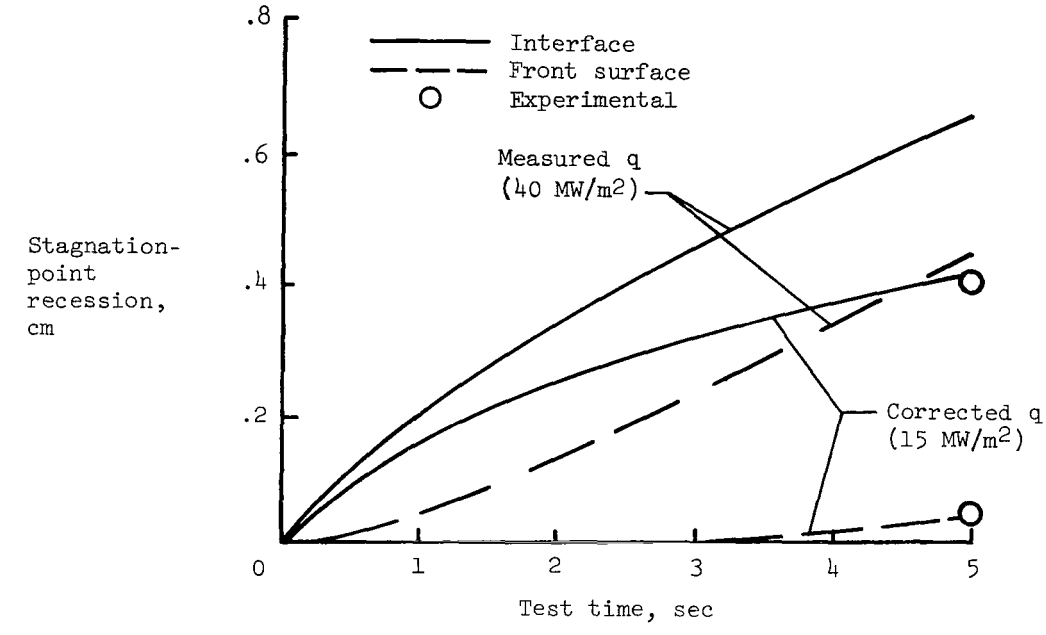

(a) Air; p = 1 atm.

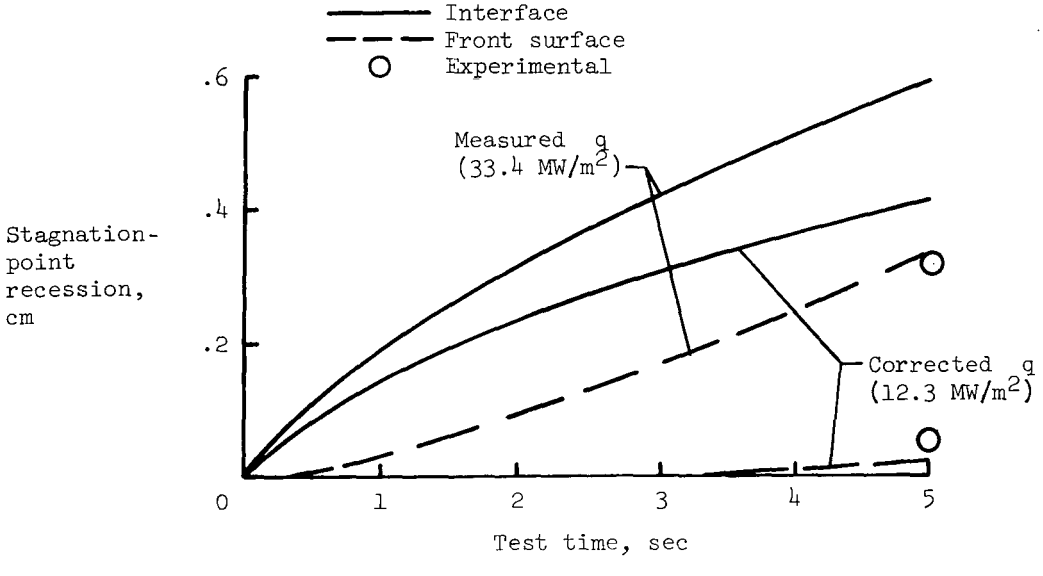

(b) Air; p = 0.3 atm.

Figure 13.- Experimental and calculated recessions for low-density phenolic nylon in carbon-arc facility.

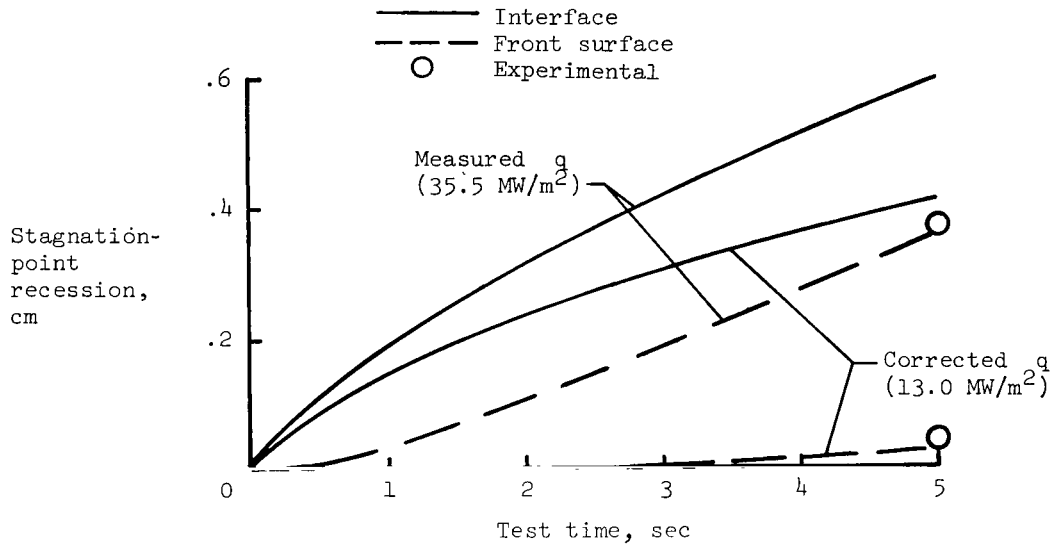

(c) Air; p = 3.0 atm.

Figure 13.- Concluded.

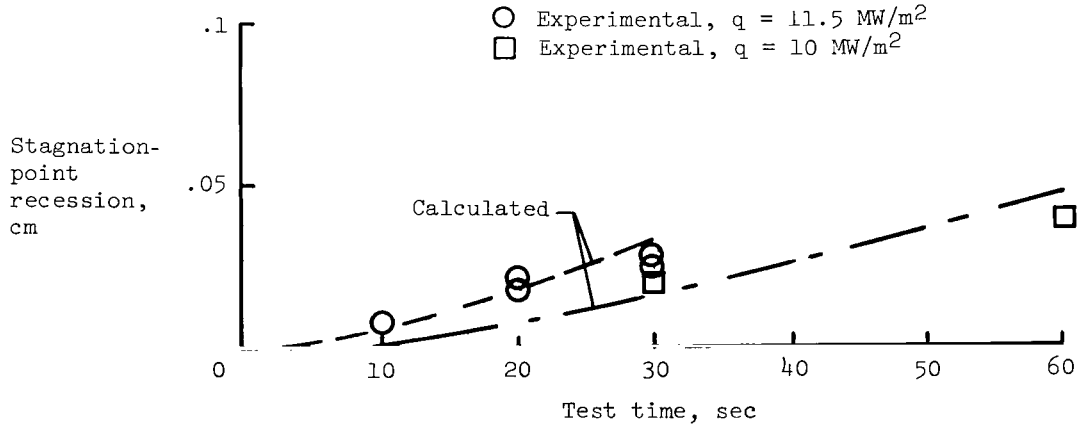

Figure 14.- Experimental and calculated recessions for graphite in xenon-arc facility. Air; p = 1 atm.

719 001 C1 U D 760820 S00903DS
DEPT OF THE AIR FORCE
AF WEAPONS LABORATORY
ATTN: TECHNICAL LIBRARY (SUL)
KIRTLAND AFB NM 87117

"The aeronautical and space activities of the United States shall be conducted so as to contribute . . . to the expansion of human knowledge of phenomena in the atmosphere and space. The Administration shall provide for the widest practicable and appropriate dissemination of information concerning its activities and the results thereof."

—NATIONAL AERONAUTICS AND SPACE ACT OF 1958

NASA SCIENTIFIC AND TECHNICAL PUBLICATIONS

TECHNICAL REPORTS: Scientific and technical information considered important, complete, and a lasting contribution to existing knowledge.

TECHNICAL NOTES: Information less broad in scope but nevertheless of importance as a contribution to existing knowledge.

TECHNICAL MEMORANDUMS: Information receiving limited distribution because of preliminary data, security classification, or other reasons. Also includes conference proceedings with either limited or unlimited distribution.

CONTRACTOR REPORTS: Scientific and technical information generated under a NASA contract or grant and considered an important contribution to existing knowledge.

TECHNICAL TRANSLATIONS: Information published in a foreign language considered to merit NASA distribution in English.

SPECIAL PUBLICATIONS: Information derived from or of value to NASA activities. Publications include final reports of major projects, monographs, data compilations, handbooks, sourcebooks, and special bibliographies.

TECHNOLOGY UTILIZATION PUBLICATIONS: Information on technology used by NASA that may be of particular interest in commercial and other non-aerospace applications. Publications include Tech Briefs, Technology Utilization Reports and Technology Surveys.

Details on the availability of these publications may be obtained from:

SCIENTIFIC AND TECHNICAL INFORMATION OFFICE

NATIONAL AERONAUTICS AND SPACE ADMINISTRATION

Washington, D.C. 20546